Tropical Cyclone Structure and Intensity Change Related to Eyewall Replacement Cycles and Annular Storm Formation, Utilizing Objective Interpretation of Satellite Data and Model Analyses

James P. Kossin
Cooperative Institute for Meteorological Satellite Studies
University of Wisconsin–Madison
1225 W. Dayton St., Room 205
Madison, WI 53706
phone: (608) 265-5356 fax: (608) 262-5974 email: kossin@ssec.wisc.edu

David S. Nolan
Division of Meteorology and Physical Oceanography
Rosenstiel School of Marine and Atmospheric Science
University of Miami
4600 Rickenbacker Causeway
Miami, FL 33149
phone: (305) 421-4930 fax: (305) 421-4696 email: dnolan@rsmas.miami.edu

Award Number: N00014-07-1-0163 (Kossin), N00014-07-1-0164 (Nolan)

LONG-TERM GOALS

This project aims toward increasing our understanding of the dynamics of secondary eyewalls in tropical cyclones and our ability to forecast their formation and associated intensity changes. This is being accomplished through a synergistic combination of theoretical, empirical, and numerical modeling approaches. We expect to apply our results to the construction of objective algorithms that will be transitioned to operations to provide forecasters with new tools for improved forecasting of tropical cyclone structure and intensity.

OBJECTIVES

1) Elucidate the internal vortex dynamics associated with secondary eyewall formation (SEF) with a unique combination of basic theory, idealized models, and full-physics models.
2) Identify and quantify the environmental factors related to SEF through application of reanalysis fields and satellite imagery.
3) Construct objective algorithms to diagnose SEF (and associated intensity changes) in real-time.

APPROACH

We are following a multi-pronged approach that incorporates basic theory, idealized modeling, full-physics modeling, and empirical/statistical analyses. Guidance for the empirical/statistical analyses is derived from the basic theory and idealized modeling results. The results of the empirical/statistical analyses then provide guidance for a systematic suite of full-physics modeling experiments. Our empirical/statistical approach involves composite analyses and Principal Component Analyses (PCA)

Report Documentation Page

Form Approved
OMB No. 0704-0188

1. REPORT DATE	2. REPORT TYPE	3. DATES COVERED
30 SEP 2008	**Annual**	**00-00-2008 to 00-00-2008**

4. TITLE AND SUBTITLE

Tropical Cyclone Structure And Intensity Change Related To Eyewall Replacement Cycles And Annular Storm Formation, Utilizing Objective Interpretation Of Satellite Data And Model Analyses

5a. CONTRACT NUMBER

5b. GRANT NUMBER

5c. PROGRAM ELEMENT NUMBER

6. AUTHOR(S)

5d. PROJECT NUMBER

5e. TASK NUMBER

5f. WORK UNIT NUMBER

7. PERFORMING ORGANIZATION NAME(S) AND ADDRESS(ES)

University of Wisconsin-Madison,Cooperative Institute for Meteorological Satellite Studies,1225 W. Dayton St., Room 205,Madison,WI,53706

8. PERFORMING ORGANIZATION REPORT NUMBER

9. SPONSORING/MONITORING AGENCY NAME(S) AND ADDRESS(ES)

10. SPONSOR/MONITOR'S ACRONYM(S)

11. SPONSOR/MONITOR'S REPORT NUMBER(S)

12. DISTRIBUTION/AVAILABILITY STATEMENT

Approved for public release; distribution unlimited

13. SUPPLEMENTARY NOTES

14. ABSTRACT

This project aims toward increasing our understanding of the dynamics of secondary eyewalls in tropical cyclones and our ability to forecast their formation and associated intensity changes. This is being accomplished through a synergistic combination of theoretical, empirical, and numerical modeling approaches. We expect to apply our results to the construction of objective algorithms that will be transitioned to operations to provide forecasters with new tools for improved forecasting of tropical cyclone structure and intensity.

15. SUBJECT TERMS

16. SECURITY CLASSIFICATION OF:			17. LIMITATION OF ABSTRACT	18. NUMBER OF PAGES	19a. NAME OF RESPONSIBLE PERSON
a. REPORT	b. ABSTRACT	c. THIS PAGE			
unclassified	**unclassified**	**unclassified**	**Same as Report (SAR)**	**13**	

of storm-centered environmental fields and satellite imagery. We have developed an objective classification scheme that diagnoses and forecasts SEF. The classification algorithm was developed in a Bayesian framework. The idealized modeling part of this work has utilized a diagnostic model based on the Eliassen transverse circulation model. The diagnostic analyses using the Eliassen model have been extended to unsteady dynamics using a time-dependent, nonhydrostatic model of symmetric vortex dynamics. The full-physics modeling part of this project is underway and involves idealized simulations of tropical cyclones designed to reproduce eyewall replacement cycles and related processes.

WORK COMPLETED

Two papers were published in 2008:

Rozoff, C. M., W. H. Schubert, and J. P. Kossin, 2008: Some dynamical aspects of tropical cyclone concentric eyewalls. *Q. J. R. Meteorol. Soc.*, **134**, 583–593.
Available here:
http://www.ssec.wisc.edu/~kossin/articles/Rozoff_QJRMS_2008.pdf

Kossin, J. P., and M. Sitkowski, 2008: An objective model for identifying secondary eyewall formation in hurricanes. *Mon. Wea. Rev.*, in press.
Available here:
http://www.ssec.wisc.edu/~kossin/sharedfiles/Kossin_Sitkowski_2008_MWR_single_spaced.pdf

Kossin and Sitkowski (2008) was selected as a *Paper of Note* by the Senior Editor of BAMS, and a description will appear in the November issue of BAMS.

A real-time prototype of the new empirical model described in Kossin and Sitkowski (2008) is presently running in-house at CIMSS.

WRF numerical simulations of eyewall replacement cycles are underway, and analysis of model output has commenced.

RESULTS

a) Theory and idealized modeling results

i. Idealized aspects of concentric eyewalls

In Rozoff et al. (2008), we investigated the role of the radial distribution of inertial stability and diabatic heating changes on the transverse circulation associated with eyewall replacement cycles (ERCs). Assuming an axisymmetric, barotropic vortex and dividing the tropical cyclone into five regions (i.e., eye, inner eyewall, moat, outer eyewall, and far-field), analytical solutions were obtained. It was found that subsidence associated with the outer eyewall does not suppress the inner eyewall. Instead, the results suggest subsidence and the resulting warming in the moat are strongly enhanced with increasing inertial stability during the strengthening and contraction of an outer eyewall. This result constitutes a new paradigm. The conventional paradigm describes the outer eyewall monopolizing low-level inflow of moist energy while inward-directed upper-level exhaust from the outer eyewall directly suppresses convection in the primary eyewall. This process is dominated by the secondary circulation. Here we showed that the primary circulation associated with the outer eyewall affects the inner eyewall by locally increasing inertial stability and thereby constraining the outflow from the inner eyewall. We also showed that the diabatic heating associated with the inner eyewall more efficiently warms the storm's core than the diabatic heating associated with the outer eyewall. Therefore, as heating shifts from an inner eyewall to an outer eyewall, a hurricane undergoing an ERC temporarily loses its ability to produce an intense, localized warm core.

In order to explore the generality of the barotropic results, we have relaxed the assumptions in Rozoff et al. (2008) to now include baroclinity and variable background static stability. To this end, we have utilized the linearized, three-dimensional anelastic vortex model described in Nolan et al. (2007) to study moat subsidence in baroclinic vortices. Although the nonhydrostatic model produces time-evolving solutions, Nolan and Grasso (2003) showed that it can also reproduce a quasi-balanced response similar to that produced by a balance model (such as used by Rozoff et al. 2008, above) when forced with a steady heat (or momentum) source. For example, using the tangential wind profile in Fig. 1a, we find that the nonhydrostatic model generates a steady transverse circulation after about 6 h of steady heating. Figure 1b compares the radial distribution of vertical motion between the analytical and numerical solutions. The solutions are nearly identical, confirming the nonhydrostatic model's utility in addressing more realistic hurricane-like vortices.

(a) **(b)**

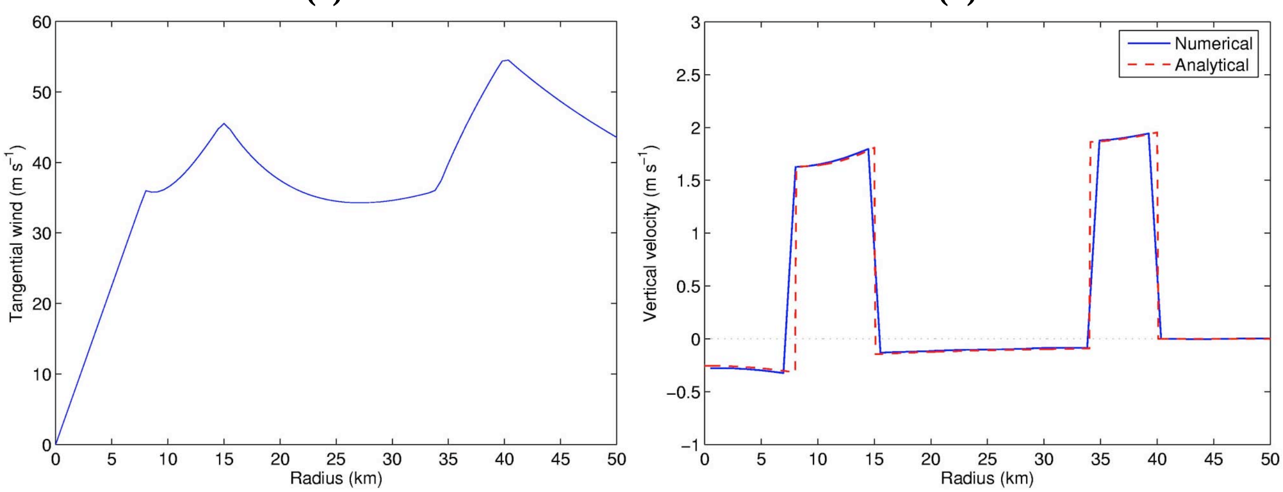

Figure 1. (a) Tangential velocity (m s^{-1}) profile used for the idealized barotropic concentric eyewall and (b) vertical motion (m s^{-1}) from the numerical solution (solid blue) and the analytical solution in Rozoff et al. (2008) at z = 5.9 km.

To investigate the impact of baroclinity and variable static stability on the transverse circulation, the nonhydrostatic model has been initialized with numerous background wind and perturbation potential temperature fields, such as the ones shown in Figs. 2a,b. These fields are in hydrostatic and gradient wind balance. The inner and outer eyewall diabatic heating prescribed in Rozoff et al. (2008) is again applied to the baroclinic vortex. Letting the model evolve in time for a variety of initial conditions with persistent forcing provides transverse circulation solutions that qualitatively resemble the analytical solutions from the barotropic vortices. However, Fig. 3 shows the difference field in vertical velocity between the barotropic vortex indicated in Fig. 1a and the baroclinic vortex in Fig. 2 after 16 h of evolution. Baroclinity constrains the secondary flow to higher levels. This is simply a consequence of the decreased inertial stability aloft and the increased static stability at low to mid-levels of the atmosphere. Nonetheless, baroclinity does not change the importance of the evolving radial distribution of inertial stability during a typical ERC.

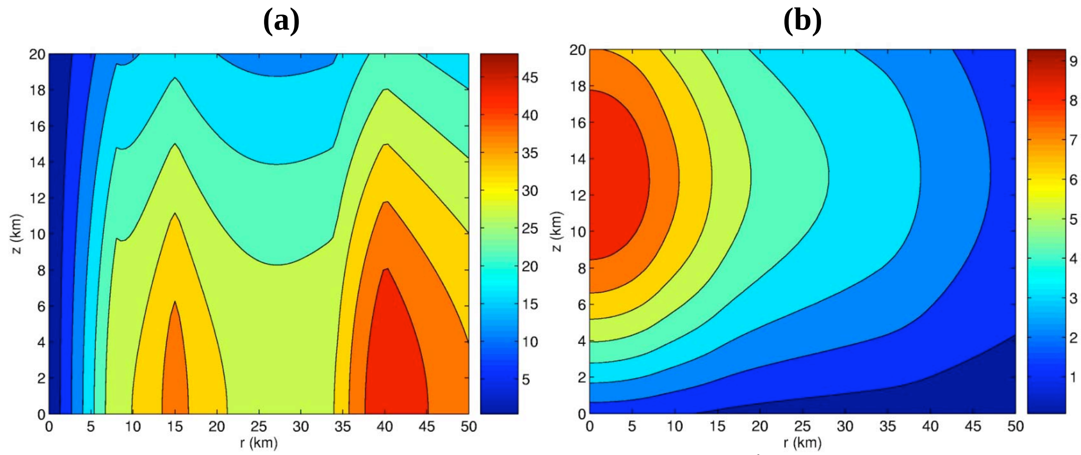

Figure 2. Radial-height cross-sections of (a) tangential wind (m s^{-1}) for the baroclinic vortex and (b) the associated potential temperature anomaly (K) field.

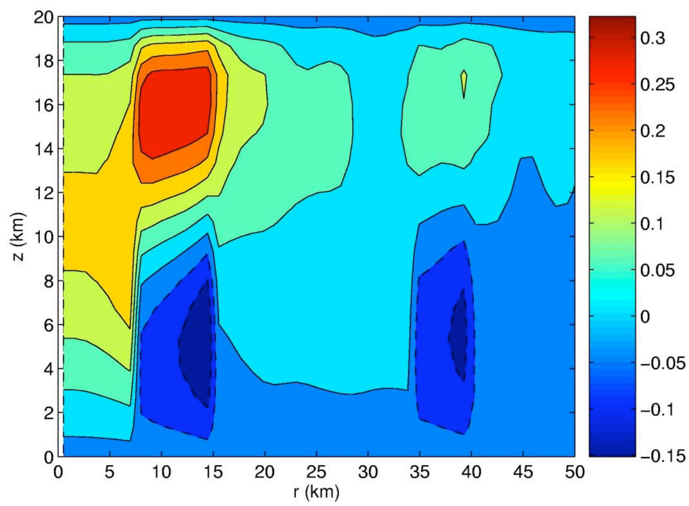

Figure 3. Radial-height cross-section of the difference field of vertical motion between the baroclinic and barotropic vortices.

ii. Numerical mesoscale simulations of eyewall replacement cycles

Using the Weather Research Forecast (WRF) model (Skamarock et al. 2005), we are currently investigating details of three-dimensional, cloud-resolving simulations of hurricanes undergoing ERCs. Our efforts include a case study of Hurricane Isabel (2003) and a suite of idealized experiments. We seek to elucidate the internal dynamical connections of ERCs and eye size with key environmental predictors discovered in Kossin and Sitkowski (2008). We anticipate secondary eyewall formation (SEF) is more likely in an environment characterized by higher potential intensity conditions, enhanced mid-to-upper level relative humidity, and minimal vertical shear. Our range of idealized experiments are designed to specifically address how simulated SEF varies with changes in thermodynamic conditions with a focus on sea-surface temperatures, relative humidity and dynamical aspects of the primary vortex. Furthermore, it is of interest to understand how the spatial distribution of favorable versus less favorable sea-surface temperatures may potentially determine the vigor and spatial extent of rainband activity and, therefore, the development of concentric eyewalls. A key question to address is whether SEF is merely an accidental creation of independent, internal dynamics, or more likely, a result of environmental conditions forcing or facilitating internal dynamics central to SEF and/or annular hurricane formation.

In the past year, we have developed two sets of model simulations that produce SEFs and ERCs. The first set are real-data simulations of Hurricane Isabel (2003). The simulations cover the period from 00 UTC 12 Sept. 2003 to 00 UTC 16 Sept. 2003, while Isabel was at or near category 5 intensity, during which the eyewall diameter and radius of maximum winds were observed to increase significantly. The initial and boundary conditions were interpolated from the analyses of the GFDL Hurricane Prediction System; the bogus vortex interpolated into the GFDL analysis allowed the simulations to be initialized near category 5 strength. The simulations use 3 nested grids with 12, 4, and 1.33 km resolution, and 40 vertical levels. Papers documenting these simulations (but not addressing the SEFs) have recently been submitted (Nolan et al. 2008a,b).

Figure 4 shows the overall evolution of one of the Isabel simulations in terms of minimum surface pressure, maximum azimuthal mean 10-m tangential winds (which are lower than the absolute maximum wind), and the radius of maximum azimuthal mean tangential wind (RMW). As seen in the Hovmöller diagram of vertical motion in Fig. 5a, an ERC takes place during the period roughly ranging from 70 to 85 h. While this eyewall cycle is somewhat interesting in that the change in minimum surface pressure and maximum wind are not very significant, this event leads to a larger eye and a substantially broadened wind field.

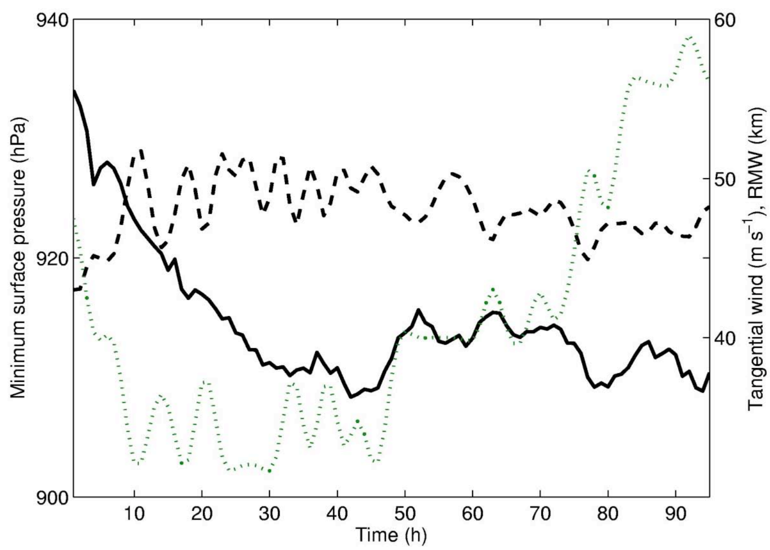

Figure 4. The time-evolution of the minimum sea-level pressure (hPa; solid), maximum azimuthal mean tangential wind (m s^{-1}; dashed) at 10-m height, and the radius of maximum mean tangential wind (km; dotted green).

We are currently investigating the axisymmetric aspects of ERCs. As seen in Fig. 5a, the azimuthal mean vertical velocity field does not clearly indicate low-level subsidence in the moat as the ERC progresses — subsidence is restricted to mid and high levels in this time frame. The surface-based convective available potential energy (CAPE) (Fig. 5b) does show that instability is depressed in the moat between the eyewalls, which is partially a consequence of increasingly stable lapse rates, a reflection of a spreading warm core and, in that regard, is consistent with the balanced vortex theory overviewed earlier. The expansion of the warm core, as indicated in the azimuthal mean difference field of potential temperature between 75 and 60 h, is shown in Fig. 6a. Figures 6c-d provide the evolution of inertial stability and the transverse circulation.

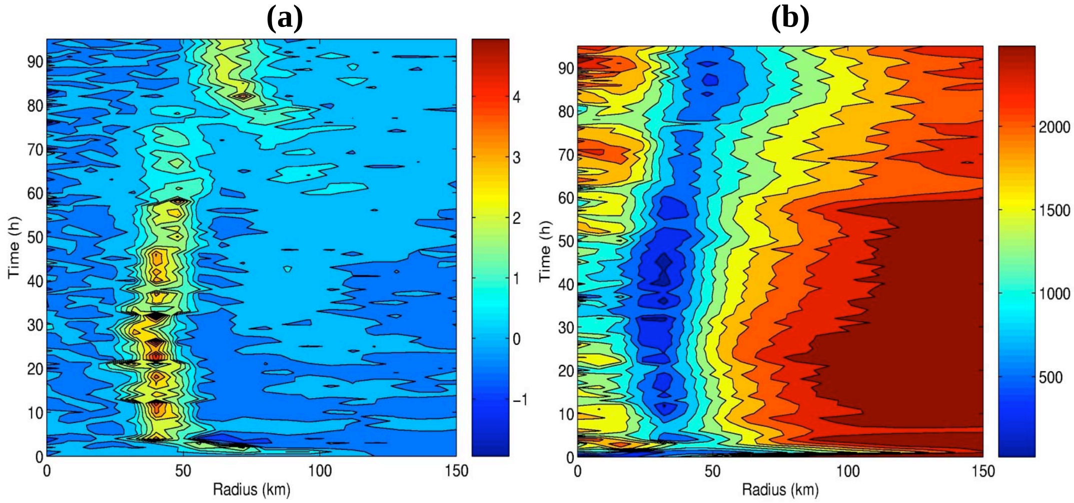

Figure 5. Radius-time Hovmoller diagarams of (a) vertical motion (m s^{-1}) at z = 3.5 km, (b) surface-based CAPE (J kg^{-1}).

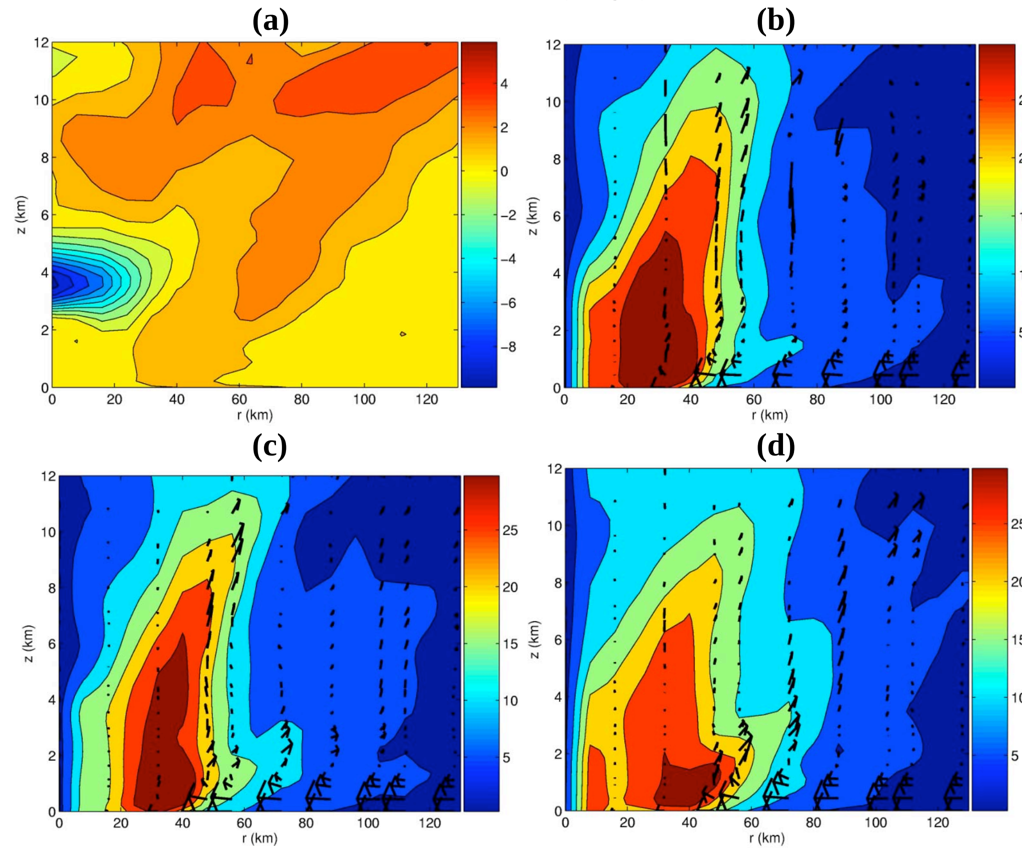

Figure 6. (a) The difference field of the azimuthal mean potential temperature (K) between 75 and 60 h and (c), (b), and (d) inertial stability and wind vectors associated with the transverse circulation at 60, 75, and 80 h.

The idealized simulations are similar in design to the recent study of Nolan (2007), using observed thermodynamic soundings from the Atlantic hurricane season. A weak, mid-level vortex is embedded in a mean flow and/or mean shear flow on the *f*-plane. A large outer domain is used with 18 km resolution, with nested grids of 6 and 2 km resolution follwing the vortex. The vortex evolves into a rapidly intensifying tropical cyclone which then reaches a quasi-steady state after about 3 days. Unfortunately, only one such simulation (e.g., Fig. 7) so far has shown a clear example of SEF and ERC; whether or not this occurs seems to be sensitive to many factors, such as the size of the initial vortex, the latitude, and even the choice of boundary layer parameterization. More simulations are currently underway to determine which of these factors are most strongly controlling the results.

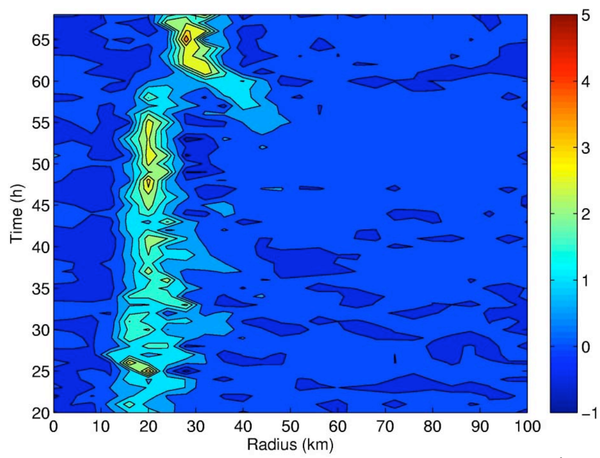

Figure 7. Radius-time Hovmoller diagarams of vertical motion (m s^{-1}) at z = 3.5 km in the idealized experiment.

As the idealized model runs are currently completing, we have made considerable progress in designing the tools to analyze leading hypotheses of SEF in the Isabel and idealized simulations. One recent and intriguing hypothesis involves the upward cascade of convectively generated potential vorticity and kinetic energy in a region outside the primary eyewall characterized by a favorable PV gradient and persistent convective clouds (Terwey and Montgomery 2008). For example, Fig. 8 shows an overall upward trend in Isabel's mass-weighted perturbation kinetic energy spectrum at most wavenumbers for a radial region outside of the RMW before, during, and immediately after concentric eyewall formation. In the hypothesis of Terwey and Montgomery, the axisymmetrization of the convectively induced PV and kinetic energy anomalies is thought to constructively combine with a wind-moisture feedback process at the air-sea interface, in a manner similar to the axisymmetric evolution described in Nong and Emanuel (2003). An even more recent hypothesis involves the response of the flow to the application of heating from an asymmetric, principle rainband surrounding a symmetric, balanced vortex (Moon 2008), which shows evidence of enhanced tangential flow in the annular region containing diabatic heating. With a particular interest in wave-mean flow interactions, we are addressing these hypotheses through potential vorticity, energy, and isentropic momentum budgets.

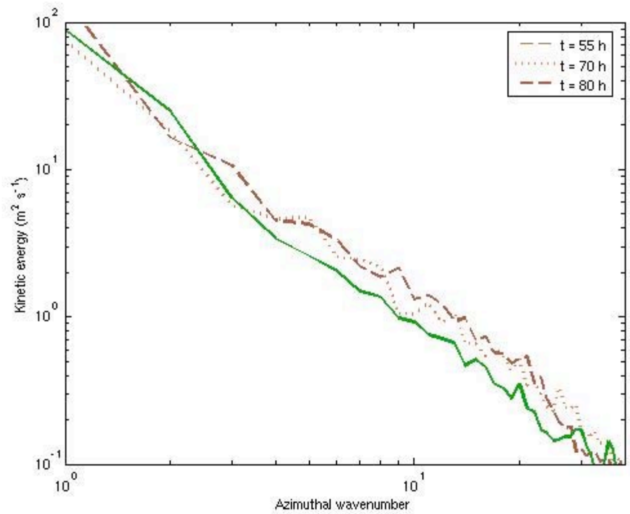

Figure 8. Mass weighted kinetic energy spectrum for the annular region extending from the radius of maximum winds to a radius of 150 km at 55, 71, and 80 h.

b) Empirical/statistical results; the new secondary eyewall formation model

We have completed the construction of a new probabilistic model that diagnoses and forecasts secondary eyewall formation. This is a significant step given the known effect that secondary eyewall formation has on storm structure and intensity, and the complete absence of any prior objective tool that can diagnose or predict these events. The skill demonstrated by our new model suggests that the mean axisymmetric environmental conditions and satellite-derived cloud structures centered on each hurricane do contain measurably useful information for estimating the probability of secondary eyewall formation. The model is based on an empirical Bayesian probabilistic model that uses environmental features as input. The features are a combination of storm-based variables such as current intensity and latitude, environmental variables such as vertical wind shear and middle- to upper-level relative humidity, and geostationary satellite infrared-based variables.

We found that secondary eyewall formation is associated with higher maximum potential intensity, lower vertical wind shear, weaker upper-level zonal winds, a deep layer of underlying warm water, and higher middle- to upper-level relative humidity (Table 1). The relationship with higher relative humidity agrees well with the numerical findings of Nong and Emanuel (2003), and with the basic idea that organized convection in the tropics is sensitive to humidity and dry air entrainment above the boundary layer (e.g. Ooyama 1969). The higher MPI suggests that secondary eyewall formation is favored in an environment that is more thermodynamically supportive of persistent deep convection. In typical tangential wind fields in hurricanes, the radial gradient of angular velocity will inherently tend to organize asymmetric convection into a circular ring. The sensitivity of secondary eyewall formation to shear may be an indication that the shear disrupts this symmetrization process, although the relationship between convection and shear is significantly more complicated (e.g., Kwon and Frank 2008). The relationship with 200 hPa zonal wind suggests that secondary eyewall formation prefers quiescent upper-levels in addition to low shear. The colder and more axisymmetric satellite brightness temperature fields are also reconcilable with the preference for stronger storms in a low-shear environment to form secondary eyewalls.

Table 1: Features applied to the Bayes probabilistic model.

Description	Preference for secondary eyewall formation
Current intensity	Stronger
Latitude	Further south
Climatological depth of 26°C ocean isotherm	Deeper
200 hPa zonal wind (200-800km from center)	Weaker (near zero), very narrow range
500-300 hPa relative humidity	Moister
0-600km average symmetric tangential wind at 850 hPa from NCEP analysis	Stronger
Azimuthally averaged surface pressure at outer edge of vortex	Lower
850-200 hPa shear magnitude	Weaker, narrow range
Maximum potential intensity	Higher, very narrow range
Standard deviation (from axisymmetry) of infrared brightness temperature between 100–300 km	Smaller (more axisymmetric)
Average infrared brightness temperature between 20–120 km	Colder, narrow range

We also considered satellite-based features constructed from a principal component analysis of storm-centered azimuthally-averaged infrared brightness temperature profiles derived from the HURSAT dataset available at the NOAA National Climatic Data Center (Knapp and Kossin 2007; Kossin et al. 2007a,b). The eigenmodes of the analysis describe varying radial structures of the average storm-centered brightness temperature, and the expansion coefficients associated with the eigenmodes were considered as potential features. We found that the expansion coefficient associated with the radial structure described by the fourth leading eigenmode was most useful for increasing the skill of the model. This eigenmode explains only 2% of the azimuthally-averaged brightness temperature variation but was found to consistently improve model performance in both ocean basins. The radial structure of this eigenmode has a local amplitude maximum beyond ~100 km from hurricane center and may be capturing anomalous subsidence warming of the upper-level cirrus shield in this region. This may be related to increased inertial stability caused by local acceleration of the tangential wind often associated with a secondary eyewall (Rozoff et al. 2008), but this relationship between brightness temperature and storm dynamics is still uncertain.

Table 2: Four 2 × 2 contingency tables for classification of secondary eyewall formation events in the North Atlantic. The top 2 × 2 table is based on the climatological probability of secondary eyewall formation. The next table is based on the probability estimated from our new algorithm using current intensity as the sole feature. The next table shows how the inclusion of the environmental features improves the algorithm performance. The bottom table is based on the addition of the satellite-derived features. All values are based on cross-validation of the model.

Forecast		**Observed** YES	**Observed** NO
Climatology	YES	0 (hits)	0 (false alarms)
	NO	129 (misses)	936 (correct negatives)
Current intensity only	YES	17	15
	NO	112	921
Current intensity plus environmental	YES	29	20
	NO	100	916
Current intensity plus environmental plus satellite	YES	39	21
	NO	90	915

Table 3: ***Performance metrics of the model.***

	Brier Skill Score	Peirce Skill Score	Briggs & Ruppert Skill Score	Probability of Detection	False Alarm Rate	Area under ROC curve
Climatology	0%	0%	0%	0%	0%	0.50
Current intensity only	12%	12%	2%	13%	2%	0.77
Current intensity plus environmental	18%	20%	7%	22%	2%	0.86
Current intensity, environment, satellite	21%	28%	14%	30%	2%	0.86

Our new model is based on the Bayes probabilistic model. The probability of secondary eyewall formation conditional on the features **F** (or, equivalently, the probability of secondary eyewall formation when a particular set of features **F** is observed) can be described by

$$P(C_{\text{yes}}|\mathbf{F}) = \frac{P(C_{\text{yes}})P(\mathbf{F}|C_{\text{yes}})}{P(\mathbf{F})} . \quad (1)$$

The cross-validated performance characteristics of the probabilistic model are summarized in Tables 2 and 3, and show the model to be measurably skillful. The cross validation was based on a leave-one-year-out method applied to 10 years of data.

Our model provides a probability, which can then be subjected to any decision rule to form a classification assignment. But in an operational hurricane-forecasting environment, the model would most likely be used in the same manner that other models – empirical or numerical – are used. That is, the forecaster can assess the evolution of the probability of secondary eyewall formation in real time, and form an expert judgment based on a variety of available information and a working knowledge of the traits and behaviors of the models being considered. An example of the model behavior in individual storms is shown in Fig. 9.

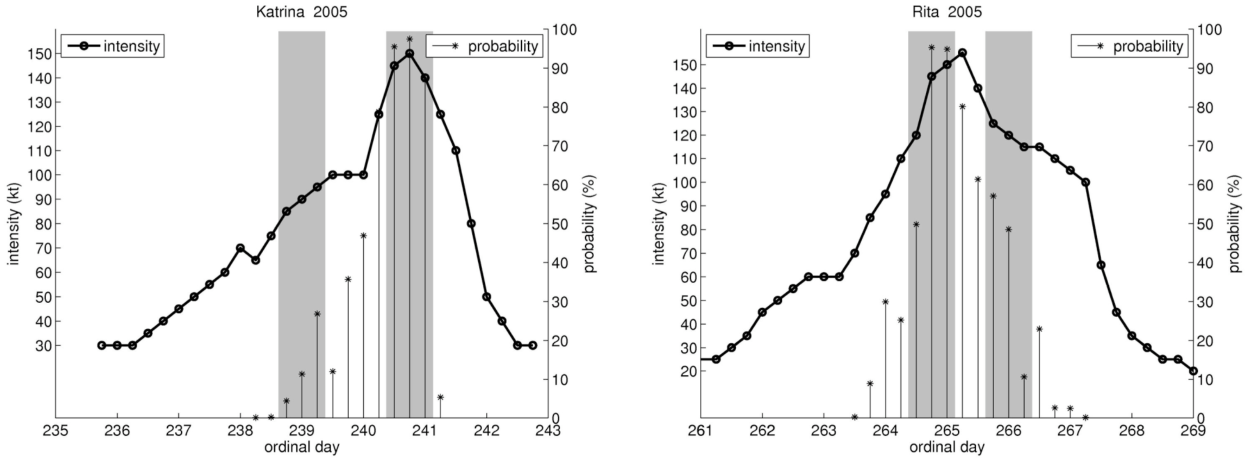

Figure 9: Evolution of current intensity (solid black line, left axis) and model-estimated probability of secondary eyewall formation (stem plot, right axis) in Hurricanes Katrina (2005), and Rita (2005). Each gray shaded region denotes a period that a secondary eyewall formation event was observed within. The model does not assign a probability when intensity is less than 65 kt (33 m s^{-1}) or when the storm center is over land.

IMPACT/APPLICATIONS

Our theoretical and idealized modeling results are uncovering the relevant dynamics of the tropical cyclone transverse circulation as it relates to the presence of secondary eyewalls. We expect this to provide invaluable guidance for initializing the full-physics numerical simulations that will continue during the final year of this project. In addition to providing further guidance for numerical simulations, our new probabilistic model provides an objective tool that has excellent potential for future transition to operations. The model is being presently considered for transition to the National Hurricane Center through the Joint Hurricane Testbed program, and we expect the potential for transition to the Joint Typhoon Warning Center to be high as well. This will be discussed further at the next Interdepartmental Hurricane Conference in St. Petersburg, FL.

RELATED PROJECTS

Much of the database construction required for the empirical/statistical part of this project was performed by a Ph.D. student under an active NOAA grant (P.I. Kossin).

REFERENCES

Bister, M., and K. A. Emanuel, 1998: Dissipative heating and hurricane intensity. *Meteor. Atm. Phys.*, **52**, 233—240.

Knaff, J. A., T. A. Cram, A. B. Schumacher, J. P. Kossin, and M. DeMaria, 2008: Objective identification of annular hurricanes. *Wea. Forecasting*, **23**, 17-28.

Knaff, J. A., J. P. Kossin, and M. DeMaria, 2003: Annular Hurricanes. *Wea. Forecasting*, **18**, 204-223.

Knapp, K. R., and J. P. Kossin, 2007: A new global tropical cyclone data set from ISCCP B1 geostationary satellite observations. *J. of App. Remote Sensing*, **1**, 013505.

Kossin, J. P., K. R. Knapp, D. J. Vimont, R. J. Murnane, and B. A. Harper, 2007a: A globally consistent reanalysis of hurricane variability and trends. *Geophys. Res. Lett.*, **34**, L04815, doi:10.1029/2006GL028836.

Kossin, J. P., J. A. Knaff, H. I. Berger, D. C. Herndon, T. A. Cram, C. S. Velden, R. J. Murnane, and J. D. Hawkins, 2007b: Estimating hurricane wind structure in the absence of aircraft reconnaissance. *Wea. Forecasting*, **22**, 89–101.

Kossin, J. P., and M. Sitkowski, 2008: An objective model for identifying secondary eyewall formation in hurricanes. *Mon. Wea. Rev.*, in press.

Kwon, Y.C., and W.M. Frank, 2008: Dynamic Instabilities of Simulated Hurricane-like Vortices and Their Impacts on the Core Structure of Hurricanes. Part II: Moist Experiments. J. Atmos. Sci., 65, 106–122.

Moon, Y., 2008: Dynamical impacts of rotating convective asymmetries on tropical cyclones. *M.S. Thesis, University of Miami, under the supervision of D. S. Nolan*, 105 pp.

Nolan, D. S., 2007: What is the trigger for tropical cyclogenesis? *Aust. Meteorol. Mag.*, **56**, 241-266.

Nolan, D. S., and L. D. Grasso, 2003: Nonhydrostatic, three-dimensional perturbations to balanced, hurricane-like vortices. Part II: Symmetric response and nonlinear simulations. *J. Atmos. Sci.*, **60**, 2717—2745.

Nolan, D. S., Y. Moon, and D. P. Stern, 2007: Tropical cyclone intensification from asymmetric convection: Energetics and efficiency. *J. Atmos. Sci.*, **64**, 3377—3405.

Nolan, D. S., D. P. Stern, and J. A. Zhang, 2008: Evaluation and comparison of planetary boundary layer parameterizations in tropical cyclones by directo comparison of in-sity data and high-resoluton simulations of Hurricane Isabel (2003). Part II: Inner-core boundary layer and eyewall structure. Submitted to *Mon. Wea. Rev*.

Nolan, D. S., J. A. Zhang, and D. P. Stern, 2008: Evaluation and comparison of planetary boundary layer parameterizations in tropical cyclones by directo comparison of in-sity data and high-resoluton simulations of Hurricane Isabel (2003). Part I: Initialization, track and intensity, and the outer core boundary layer. Submitted to *Mon. Wea. Rev.*

Nong, S., and K. A. Emanuel, 2003: A numerical study of the genesis of concentric eyewalls in hurricanes. *Quart. J. Roy. Meteor. Soc.*, **129**, 3323—3338.

Ooyama, K., 1969: Numerical simulation of the life cycle of tropical cyclones. J. Atmos. Sci., 26, 3–40.

Rozoff, C. M., W. H. Schubert, and J. P. Kossin, 2008: Some dynamical aspects of tropical cyclone eyewalls. *Q. J. R. Meteor. Soc.*, **134**, 583—593.

Skamarock, W. C., J. B. Klemp, J. Dudhia, D. O. Gill, D. M. Barker, W. Wang, and J. G. Powers, 2005: *A Description of the Advanced Research WRF Version 2*. NCAR technical note 468+STR, 88 pp.

Terwey, W. D., and M. T. Montgomery, 2008: Secondary eyewall formation in two idealized, full-physics modeled hurricanes. *J. Geophys. Res.*, **113**, D12112, doi:10.1029/2007JD008897.

Willoughby, H. E., J. A. Clos, and M. G. Shoreibah, 1982: Concentric eye walls, secondary wind maxima, and the evolution of the hurricane vortex. *J. Atmos. Sci.*, **39**, 395—411.

PUBLICATIONS

Rozoff, C. M., W. H. Schubert, and J. P. Kossin, 2008: Some dynamical aspects of tropical cyclone concentric eyewalls. *Q. J. R. Meteorol. Soc.*, **134**, 583–593.

Available here:
http://www.ssec.wisc.edu/~kossin/articles/Rozoff_QJRMS_2008.pdf

Kossin, J. P., and M. Sitkowski, 2008: An objective model for identifying secondary eyewall formation in hurricanes. *Mon. Wea. Rev.*, in press.
Available here:
http://www.ssec.wisc.edu/~kossin/sharedfiles/Kossin_Sitkowski_2008_MWR_single_spaced.pdf

HONORS/AWARDS/PRIZES

Kossin and Sitkowski (2008) was selected as a *Paper of Note* by the Senior Editor of the Bulletin of the American Meteorological Society, and a description will appear in the November 2008 issue of the Bulletin.